

## Determination of the mechanical properties of normal and calcified human mitral chordae tendineae

José A. Casado<sup>1</sup>, Soraya Diego<sup>1</sup>, Diego Ferreño<sup>1,\*</sup>, Estela Ruiz<sup>1</sup>, Isidro Carrascal<sup>1</sup>, David Méndez<sup>1</sup>, José M. Revuelta<sup>2</sup>, Alejandro Pontón<sup>2</sup>, José M. Icardo<sup>3</sup>, and Federico Gutiérrez-Solana<sup>1</sup>

<sup>1</sup> LADICIM - University of Cantabria, E.T.S. Ingenieros de Caminos, Canales y Puertos, Spain

<sup>2</sup> Hospital Universitario Marqués de Valdecilla, Santander, Spain

<sup>3</sup> University of Cantabria, Faculty of Medicine, Spain

\* Corresponding author: ferrenod@unican.es

**Abstract** The aim of the present research is to determine the influence of the calcification of human mitral valves on the mechanical properties of their marginal chordae tendineae. The study was performed on marginal chords obtained from thirteen human mitral valves, explanted at surgery, including six non-calcified, four moderately calcified and three strongly calcified valves. The mechanical response of the chords from the non-calcified and moderately calcified valves was determined by means of quasi-static tensile tests (the poor condition of the strongly calcified valves prevented them from being mechanically characterised). The material parameters that were obtained and analysed (the Young's modulus, the secant modulus, the proportional limit stress, the ultimate strength, the strain at fracture and the density of energy stored up to maximum load) revealed noticeable differences in mechanical behaviour between the two groups of mitral chordae tendineae. Large scatter was obtained in all cases, nevertheless, considering the mean values, it was observed that the normal chords are between three and seven times stiffer or more resistant than the moderately calcified ones. On the contrary, the results obtained for the strain at fracture showed a rather different picture as, in this case, no significant differences were observed between the two families of chords. A scanning electron microscopy study was conducted in order to find out the relevant features of the calcium deposits present in the calcified chordae tendineae. In addition, the general aspects appreciated in the stress vs. strain curves were correlated with the collagen morphological evidences determined microscopically. Finally, the calcium content present in the three groups of chords was quantitatively determined through atomic absorption spectroscopy; then, the relation between the mechanical properties of normal and moderately calcified chords as a function of its calcium content was obtained. This analysis confirmed the existence of a strong correlation between calcium content and stiffness or resistance whereas the influence on the ductility seems to be negligible.

**Keywords** mitral chordae tendineae, tensile test, calcium content, atomic absorption spectroscopy

## 1. Introduction and scope of the research

### 1.1. The mitral valve and the mitral chordae tendineae

The mitral valve (MV) is composed of four elements (see Fig. 1 (a)): the valve annulus, the valve leaflets (anterior and posterior), the mitral chordae tendineae (MCT) and the papillary muscles [23, 31, 13]. The MCT link the free edges and the ventricular surface of both leaflets of the MV to the papillary muscles, thus preventing the backflow of the blood into the left atrium during ventricular contraction. Several equivalent classifications for the MCT are proposed in the literature [13, 29, 12, 26, 27, 3, 20, 31, 24]. In general, the MCTs are classified according to their insertion sites on the mitral leaflets. In this sense, the anterior leaflet includes: (i) marginal chordae and (ii) strut chordae. The posterior leaflet has: (i) marginal chordae; (ii) basal chordae and (iii) commissural chordae. In Fig. 1 (b), a typical layout of MCT is shown [24, 17, 16, 13, 22, 24].

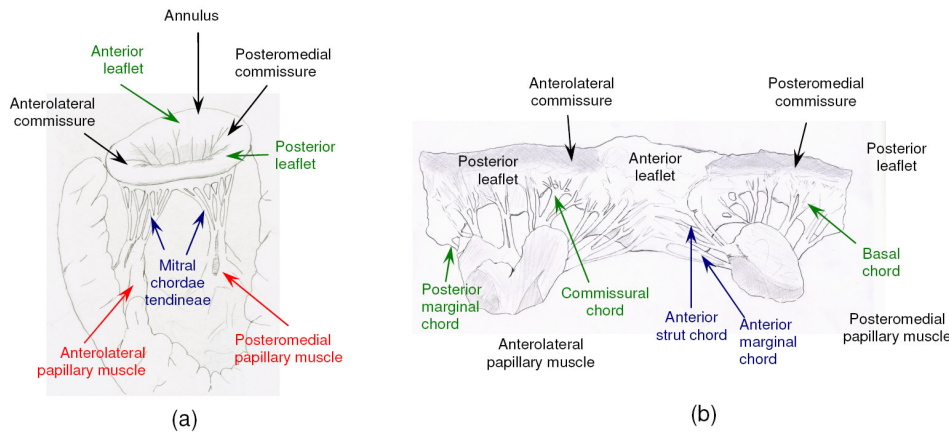


Fig. 1. Schematic drawing of the MV showing the valve leaflets, the papillary muscles and the MCT, (a), and schematic drawing of a MV as a continuous piece of tissue, (b).

## 1.2. Mitral valve calcification

Mitral regurgitation (MR) is the reflux of blood from the left ventricle into the left atrium during cardiac systole [4]. Carpentier et al. introduced a pathophysiologic classification of MR [2] based on the mitral leaflet motion. MR with normal motion is type I, with increased motion is type II and with restricted motion is type III. Heart valves are frequent locations of extensive calcium deposits, in particular because of rheumatic disease [19, 18, 6, 25].

## 1.3. Scope of the research

In this experimental study, the biomechanical properties of normal and calcified human MCT were determined. The objectives of the study are threefold: (i) to characterise (by means of quasi-static tensile tests) the mechanical behaviour of normal and calcified MCT; (ii) to quantitatively determine (through atomic absorption spectroscopy, AAS) the amount of calcium present in MCT, correlating this content with their mechanical response; (iii) to describe (through scanning electron microscopy, SEM) the relevant features associated to the fracture process and to the calcium deposits in the MCT. In the past, several studies [12, 21, 8, 16, 14, 15, 28, 10] were carried out in order to characterise the mechanical response of MCT. Nevertheless, to the knowledge of the authors, no experimental data on calcified human MCT are currently available, the present work being, therefore, the first attempt to obtain this information.

## 1.4. Material and methods

After receiving the approval of the Ethics Committee of the Marqués de Valdecilla University Hospital (Santander, Spain), the surgeons participating in the research provided a set of 13 human MVs. They classified the available MVs into three different groups: (i) 6 were obtained from patients (4 men and 2 women, aged between 36 and 63) who required heart transplant and whose MVs were not affected by any disease. The functional marginal MCT excised from these MVs constitute the control group of this study; (ii) 4 moderately calcified MVs and, (iii) 3 strongly calcified MVs, were obtained from patients who required valve replacement (1 man and 3 women, aged between 48 and 74 for the moderately calcified; 2 men and 1 women, aged between 54 and 79 for the strongly calcified Mvs). The overall appearance of the three kinds of mitral valves is shown in Fig. 2. The MVs provided by the surgeons were taken from the operating room to the mechanical laboratory in a portable refrigerator. The protocol proposed by Prot [22] was followed to preserve the integrity of the biological material.

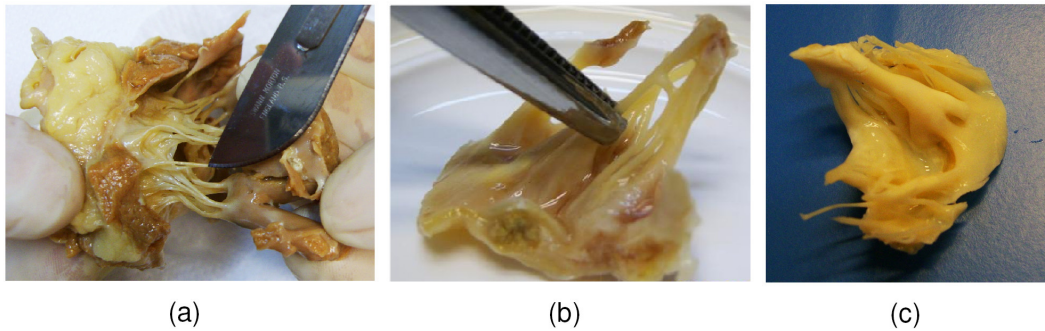


Fig. 2. General aspect of the three kinds of MVs studied in this research: (a) a healthy MV, (b) a moderately calcified MV, (c) a strongly calcified MV

## 2. Experimental techniques

The MCT were excised from the MVs preserving part of the leaflets and the papillary muscle in order to facilitate the adhesion of the specimen to the set up designed to perform the tests. To avoid the slipping of the tissue from the clamps, and adequate set up was designed and fabricated. In all cases, calibrated photographs of the specimens were taken to determine the average cross-sectional area ( $A_0$ ) and the initial gauge length ( $L_0$ ) of the specimen [13]. The tensile tests were performed under displacement control conditions, applying a constant rate of 1 mm/min following the procedure described by Ritchie [24, 7]. The stress – strain curve of each test was obtained and the relevant mechanical parameters of the material were determined: the Young’s modulus ( $E$ ), the secant modulus ( $E_s$ ), the proportional limit stress ( $\sigma_P$ ), the ultimate strength ( $\sigma_R$ ), the strain at fracture ( $\epsilon_R$ ) and the density of energy (energy per unit volume of the specimen) stored up to maximum load ( $E_a$ ). To detect the calcium deposits in the MCT, some specimens were observed by means of SEM with a JEOL JSM 5800 scanning electron microscope. AAS technique was used to determine the concentration of calcium in some selected samples [9].

## 3. Experimental results

### 3.1. Tensile tests

The force vs. elongation curve represented in Fig. 3 (a) corresponds to a tensile test performed on one of the functional MCT analysed. The figure includes a text box with the geometric dimensions of the chord as well as some relevant points (A, B, C and D, represented as solid points). The stress vs. strain curve (engineering variables) is represented in Fig. 3 (b), where the most representative mechanical parameters are included ( $E$ ,  $E_s$ ,  $\sigma_P$ ,  $\sigma_R$ ,  $\epsilon_R$  and  $E_a$ ). This example allows the general features of the mechanical response of the MCT to be appreciated:

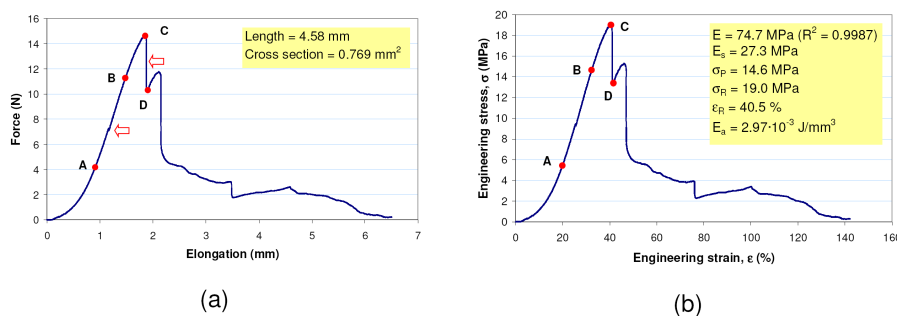


Fig. 3. Typical curve of mechanical behaviour of one of the MCT, showing the relevant features: (a) force vs. elongation; (b) stress vs. strain (engineering variables)

As stated above, one of the main aims of this research consists of comparing the mechanical response of normal and moderately calcified MCT. For this purpose, in Fig. 4, the average stress-strain curves of both families are shown, including the standard deviations. Moreover, each of the datasets was represented, see Fig. 5, using a box plot.

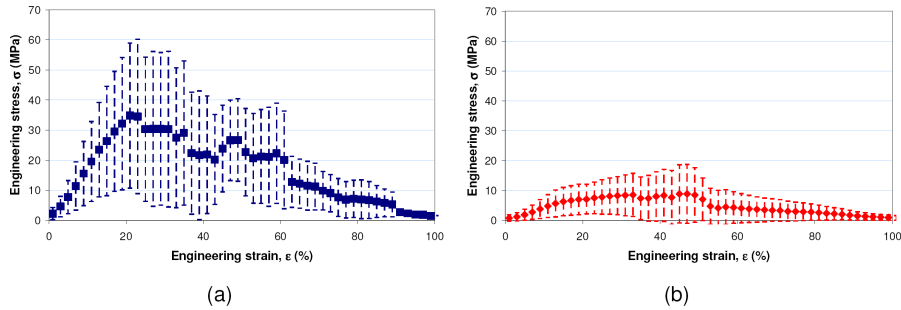


Fig. 4. Average stress-strain curve for the normal, (a), and moderately calcified, (b), chordae, including the standard deviations

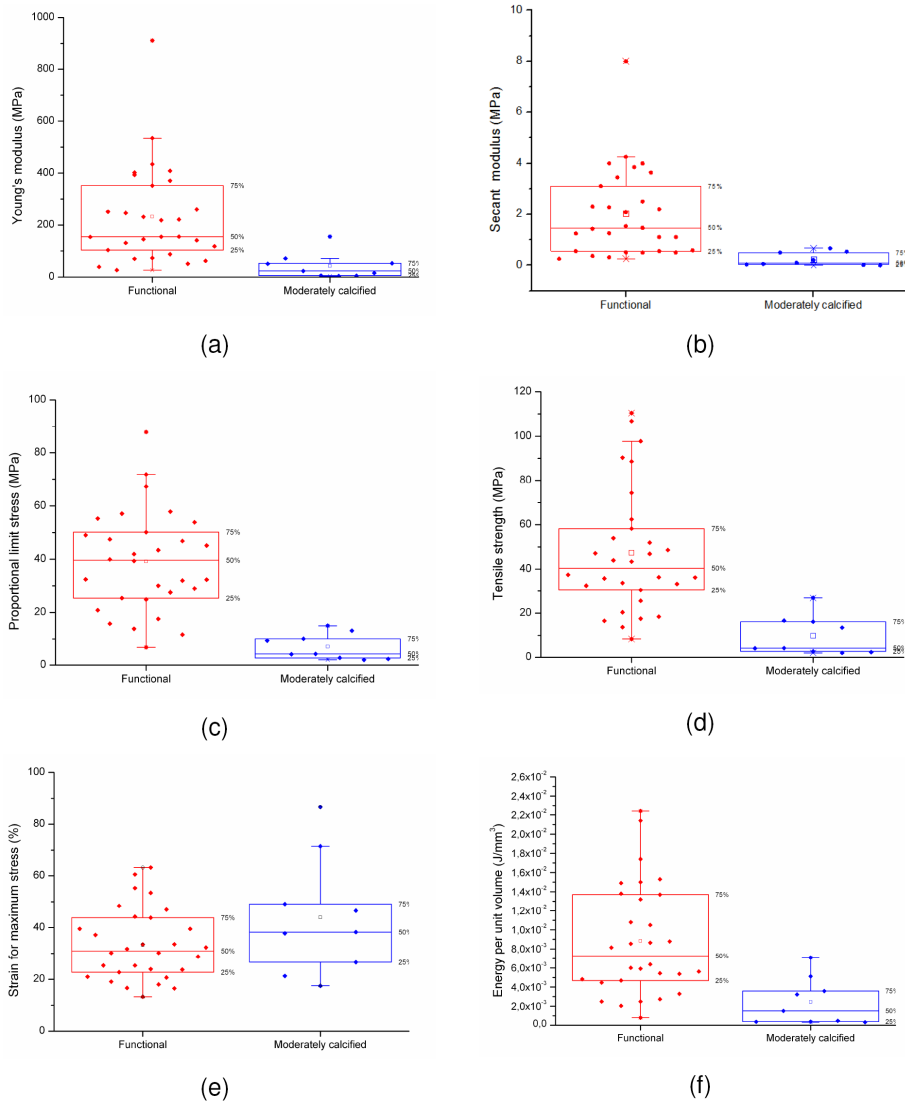


Fig. 5. Box plots representing the mechanical parameters analysed for normal and moderately calcified MCT: (a) Young's modulus; (b) secant modulus; (c) proportional limit stress; (d) tensile strength; (e) strain at fracture; (f) density of energy up to maximum load

### 3.2. SEM and EDS analysis

In Fig. 6, a comparison between a normal chord (a), a moderately calcified one (b) -both previously tested up to fracture- and one MCT obtained from one of the strongly calcified MVs available for the research (c), are shown.

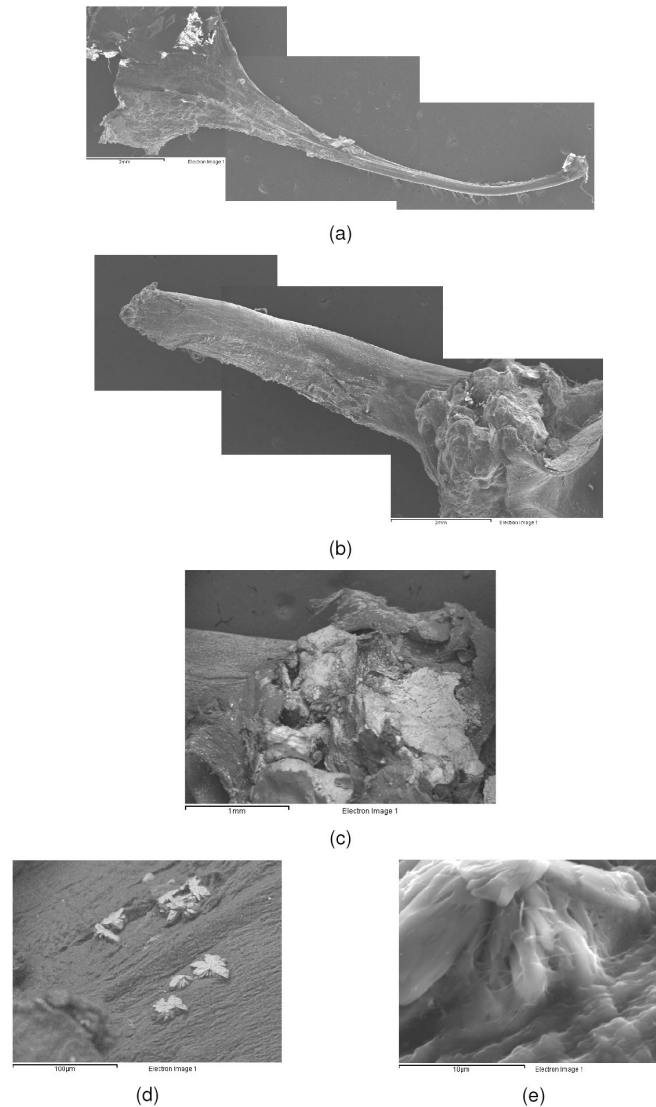


Fig. 6. Comparison through SEM between: (a) a normal, (b) a moderately calcified and (c) a strongly calcified MCT. (d) General perspective of some surface calcium deposits; (e) detail of a deposit deeply rooted in the chord.

### 3.3. Determination of the calcium content present in the chordae through atomic absorption spectroscopy

The calcium content of several MCT was determined through AAS. Specifically, the material analysed consisted of: (i) 15 MCT obtained from the 6 normal MVs, (ii) 8 MCT obtained from the 4 moderately calcified MVs and, (iii) 6 MCT obtained from the 3 strongly calcified MVs. The normal and moderately calcified chords were among those previously subjected to tensile tests (the two halves of each specimen were jointly analysed). The calcium content measured (expressed in terms of mg Ca / mg dry tissue) is represented in Fig. 7 (notice that a logarithm scale was used).

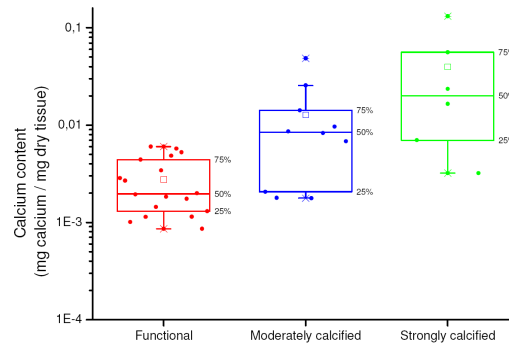


Fig. 7. Values of the calcium content measured through AAS in functional, moderately calcified and strongly calcified MCT

## 4. Discussion

### 4.1. Tensile tests

After carefully analysing the tensile curves, the following systematic characteristics were identified: i) The curves show a pronounced nonlinear behaviour in their initial region. For reduced loads, the collagen fibres are in relaxed conditions and appear wavy and crimped (Section 4.2 includes some additional microscopic information) [5, 22, 24]. ii) Next, a region of linear behaviour develops from point A to point B. The points included in this interval were used to obtain  $E$ , see Fig. 3 (b). From a microstructural point of view, the crimp patterns disappear and the collagen fibres are progressively straightened and aligned by the applied force. iii) From point B, the curve starts to bend until point C, where a sudden fracture takes place. The coordinates of point C correspond to  $\epsilon_R$  and  $\sigma_R$ . iv) In general, irregularities consisting of partial unloads were observed in the experimental curves (see the arrows in Fig. 3 (a)).

Taking into consideration the information gathered in Fig. 5, the following aspects can be drawn: i) A great difference between functional and moderately calcified MCT is appreciated when the mechanical parameters related with the stiffness ( $E$ ,  $E_s$ ) or the resistance ( $\sigma_P$ ,  $\sigma_R$  or  $E_a$ ) are considered. Indeed, observing the mean values of these parameters reveals that, on average, the normal MCT are between three and seven times stiffer or more resistant than the moderately calcified chords. ii) Although there is not enough information available to conduct a statistical analysis of the distribution of minimum values, the results clearly suggest that these are noticeably lower for the moderately calcified chords than for the functional ones, whenever the stiffness or resistant parameters ( $E$ ,  $E_s$ ,  $\sigma_P$ ,  $\sigma_R$  or  $E_a$ ) are being considered. iii) The results obtained for the strain at fracture,  $\epsilon_R$  show a rather different picture: in this case, see Fig. 5 (e), no significant differences can be seen between normal and moderately calcified MCT.

### 4.2. SEM and EDS analysis

In Section 4.1, the relevant aspects of a typical stress vs. strain curve were described and explained because of the microstructural changes that take place as a MCT is stretched. In order to confirm the validity of the above mentioned explanations, several previously tested MCT were fixed in 3% glutaraldehyde, carefully opened in longitudinal direction with the help of a scalpel, and examined by SEM. In Fig. 8, a comparison between the arrangements of collagen fibres in a non-previously tested MCT (Fig. 8 (a)), and a MCT tested up to fracture (Fig. 8 (b)) is shown. In addition, several interrupted tests were conducted to examine the validity of the explanation of the sudden unloads

detected in the experimental curves. These tests consist of stretching some chords until the first unload occurs (therefore, before the final fracture); immediately after that, the test is stopped and the chord is longitudinally opened to be examined in the SEM.

#### 4.3. Determination of the calcium content present in the chordae through atomic absorption spectroscopy

In Fig. 9, the relation between the mechanical properties of normal and moderately calcified MCT as a function of calcium content is represented (notice that a logarithm scale was used in all cases). The data included in each of the graphs were fitted through a potential law function (a linear fitting on a log-log scale) to show the trends of the different families of data. The equation of the fitting and the R-squared value are shown on a chart box. This set of figures serves to confirm some of the aspects reported previously in Section 1; thus, the influence of the calcium content is clear for the mechanical parameters  $E$ ,  $E_s$ ,  $\sigma_P$ ,  $\sigma_R$  and  $E_a$ . In contrast, the effect of the amount of calcium on the strain at fracture,  $\varepsilon_R$ , seems to be negligible.

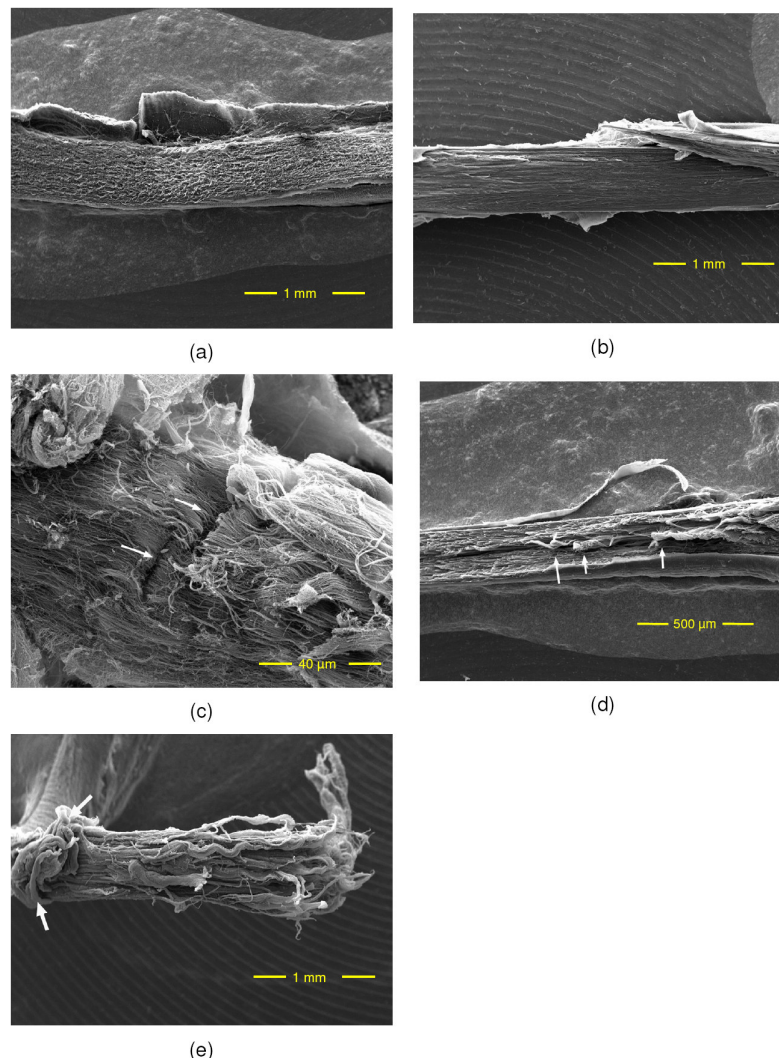


Fig. 8. SEM micrographs comparing the collagenous core of a non previously tested MCT, (a), with another chord tested up to fracture, (b). Picture (c) shows some micro-fractures detected in the collagen fibres of MCT previously subjected to interrupted tensile tests whereas in (d), the retraction of some broken fibres is appreciated (see the arrows). Micrograph (e) allows the detailed appearance of the fracture region of a MCT to be appreciated; the outer spongy layer of the chord is retracted (arrows) due to its higher elasticity.

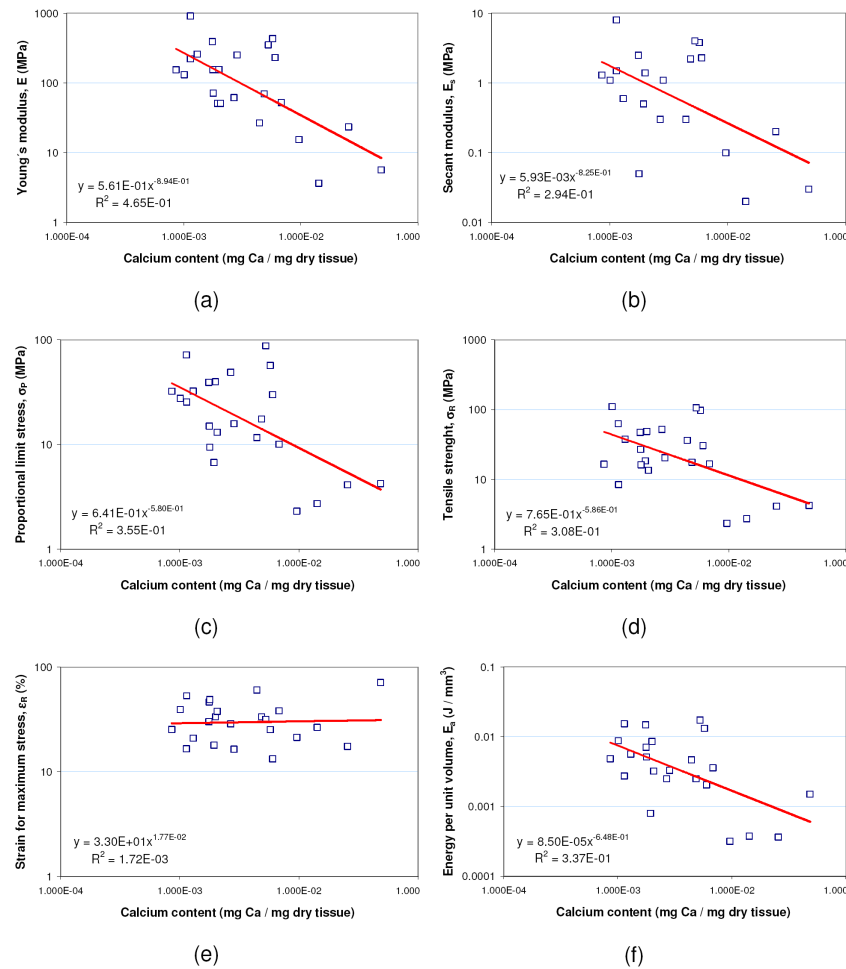


Fig. 9. Graphs representing the influence of the calcium content on the mechanical parameters analysed for normal and moderately calcified MCT: (a) Young's modulus; (b) secant modulus, (c) proportional limit stress; (d) tensile strength; (e) strain at fracture; (f) density of energy up to maximum load.

## 5. Conclusions

In general, although large scatter was systematically obtained, a great difference can be observed between functional and moderately calcified MCT when the mechanical parameters related with the stiffness (Young's modulus, secant modulus) or the resistance (proportional limit stress, ultimate strength and density of energy stored up to maximum load) are considered. In contrast, no significant differences can be seen between normal and moderately calcified MCT when comparing the strain at fracture. The amount of calcium present in normal, moderately and strongly calcified chords was measured through AAS; noticeable differences in calcium content were detected between them, although large scatter was present in the results. This analysis allowed the correlation between the measured mechanical properties and the level of calcification of normal and moderately calcified chords to be established. Finally, the relevant features associated with the fracture process and the calcium deposits in the MCT were examined with the SEM. In this sense, the calcium deposits (presumably in the form of hydroxyapatite) present in the moderately and strongly calcified chords were observed; in this latter case, some deposits of deeply rooted substances were appreciated. Moreover, several previously tested MCT together with some chords subjected to interrupted tensile tests were opened and examined in the SEM. As a result, some explanatory mechanisms were proposed in order to justify the typical aspects observed in the stress vs. strain curves.



## Acknowledgments

The authors wish to express their gratitude to the Instituto de Formación e Investigación Marqués de Valdecilla (IFIMAV) for their funding of the research. Moreover, the participation of J.M. Icardo was supported by grant CGL2008-04559/BOS from the Ministerio de Educación y Ciencia.

## References

- [1] Anyanwu, A.C., Bridgewater, B., Adams, D.H. 2010. The lottery of mitral valve repair surgery. *Heart* 96, 1964-1967.
- [2] Carpentier, A., Chauvaud, S., Fabiani, J.N., et al., 1980. Reconstructive surgery of mitral valve incompetence: ten-year appraisal. *J Thorac Cardiovasc Surg.* 79, 338-348.
- [3] David, T.E., Burns, R.J., Bacchus, C.M., Druck, M.N., 1984. Mitral valve replacement for mitral regurgitation with and without preservation of chordae tendineae. *J Thorac Cardiovasc Surg*, 88 (5 Pt 1): 718-25.
- [4] Edmunds, L.H. Jr., 1997. *Cardiac surgery in the adult*. McGraw-Hill. New York.
- [5] Fratzl, P., Misof, K., Zizak, I., Rapp, G., Amenitsch, H., Bernstorff, S., 1998. Fibrillar structure and mechanical properties of collagen. *J. Struct.Biol.* 122, 119-122.
- [6] Fulkerson, P.K., Beaver, B.M., Auseon, J.C., Graber, H.L., 1979. Calcification of the mitral annulus: etiology, clinical associations, complications and therapy. *Am J Med.* 66, 967.
- [7] Fung, Y.C., 1993. *Biomechanics. Mechanical properties of living tissues*. Springer.
- [8] He, S., Weston, M.W., Lemmon, J., Jensen, M., Levine, R.A., Yoganathan, A.P., 2000. Geometric distribution of chordae tendineae: an important anatomic feature in mitral valve function. *Journal of Heart Valve Disease* 9. 4, 495–503.
- [9] ISO 7980:1986. Water quality. Determination of calcium and magnesium. Atomic absorption spectrometric method.
- [10] Jimenez, J.H., He, S., Soerensen, D.D., He, Z., Yoganathan, A.P., 2003. Effects of a Saddle Shaped Annulus on Mitral Valve Function and Chordal Force Distribution: An In Vitro Study. *Annals of Biomedical Engineering.* 31(10), 1171-1181.
- [11] Jimenez, J.H., Soerensen, D.D., He, Z., Ritchie, J., Yoganathan, A.P, 2005. Mitral valve function and chordal force distribution using a flexible annulus model: an in vitro study. *Annals of Biomedical Engineering.* 33, 557-566.
- [12] Kunzelman, K.S., Cochran, R.P., 1990. Mechanical properties of basal and marginal mitral valve chordae tendineae. *ASAIO Transactions* 36 (3), M405–408.
- [13] Lam, J.H.C., Ranganathan, N., Wigle, E.D., Silver, M.D., 1970. Morphology of the human mitral valve chordae tendineae: a new classification. *Circulation* XLI, 449-458.
- [14] Lim, K.O., Boughner, D.R., 1975. Mechanical properties of human mitral valve chordae tendineae: variation with size and strain rate. *Canadian Journal of Physiology.* 53, 330–339.
- [15] Lim, K.O., Boughner, D.R., 1976. Morphology and relationship to extensibility curves of human mitral valve chordae tendineae. *Circulation Research* 39, 580–585.
- [16] Lomholt, M., Nielsen, S.L., Hansen, S.B., Andersen, N.T., Hasenkam, J.M., 2002. Differential tension between secondary and primary mitral chordae in an acute in-vivo porcine model. *Journal of Heart Valve Disease.* 11 (3), 337–345.
- [17] Millington-Sanders, C., Meir, A., Lawrence, L., Stolinski, C., 1998. Structure of chordae tendineae in the left ventricle of the human heart. *Journal of Anatomy.* 192, 573-581.
- [18] Nair, C.K., Aronow, W.S., Stokke, K., Mohiuddin, S.M., Thomson, W., Sketch, M.H., 1984. Cardiac conduction defects in patients older than 60 years with aortic stenosis with and without mitral annular calcium. *Am J Cardiol.* 53, 169–172.
- [19] Nair, C.K., Sketch, M.H., Ahmed, I., Thomson, W., Ryschon, K., Woodruff, M.P., et al., 1987. Calcific valvular aortic stenosis with and without mitral annular calcium. *Am J Cardiol.* 60,

865–870.

- [20] Nielsen, S.L., Timek, T.A., Green, G.R., Dagum, P., Daughters G.T., Hasenkam, J.M., Bolger, A.F., Ingels, N.B., Miller, C., 2003. Influence of Anterior Mitral Leaflet Second-Order Chordae Tendineae on Left Ventricular Systolic Function. *Circulation*. 108, 486.
- [21] Obadia, J.F., Casali, C., Chassignolle, J.F., Janier, M., 1997. Mitral subvalvular apparatus: different functions of primary and secondary chordae. *Circulation* 96 (9), 3124–3128.
- [22] Prot, V. Skallerud, B., Sommer, G., Holzapfel, G.A., 2010. On modelling and analysis of healthy and pathological human mitral valves: Two case Studies. *Journal of the mechanical behaviour of biomedical Materials*. 167-177.
- [23] Ranganathan, N., Lam, J.H., Wigle, E.D., Silver, M.D., 1970. Morphology of the human mitral valve II—the valve leaflets. *Circulation*. XLI, 459–567.
- [24] Ritchie, J.L., 2004. The material properties of the chordae tendineae of the mitral valve: an in vitro investigation. Ph.D. Georgia Institute of Technology.
- [25] Roberts, W.C., Waller, B.F., 1981. Mitral valve "anular" calcium forming a complete circle or "O" configuration: clinical and necropsy observations. *Am Heart J*. 101, 619.
- [26] Rodriguez, F., Langer, F., Harrington, K.B., et al. 2004. Importance of mitral valve second-order chordae for left ventricular geometry, wall thickening mechanics, and global systolic function. *Circulation* 14;110 (11 Suppl 1):II115-II122.
- [27] Rodriguez, F., Langer, F., Harrington, K.B. et al. 2005. Effect of cutting second-order chordae on in-vivo anterior mitral leaflet compound curvature. *J Heart Valve Dis* 14(5), 592-601.
- [28] Sedransk, K.L., Grande-Allen, K.J., Vesely, I., 2002. Failure Mechanics of Mitral Valve Chordae Tendineae. *Journal of Heart Valve Disease*. 11, 644-650.
- [29] Virmani, R., Atkinson, J.B., Forman, M.B., Rabinowitz, A.M., 1987. Mitral valve prolapse. *Hum Pathol*. 18, 596–602.
- [30] Votta, E., Arnoldi, A., Invernizzi, A., Ponzini, R., Veronesi, F., Tamborini, G., Pepi, M., Alamanni, F., Redaelli, A., Caiani, E.G., 2009. Mitral valve patient-specific finite element modelling from 3-D real time echocardiography: a potential new tool for surgical planning. MICCAI Workshop on Cardiovascular Interventional Imaging and Biophysical Modelling, CI2BM09.
- [31] Yoganathan, A. P., Lemmon, J. D., Ellis, J. T., 2000. Hard Tissue Replacement. *The Biomedical Engineering Handbook: Second Edition*. Ed. Joseph D. Bronzino, Boca Raton: CRC Press LLC.